

# Analysis of Oxidized Phospholipids by MALDI Mass Spectrometry Using 6-Aza-2-thiothymine Together with Matrix Additives and Disposable Target Surfaces

Gerald Stübiger,<sup>\*,†</sup> Omar Belgacem,<sup>‡</sup> Pavel Rehulka,<sup>§</sup> Wolfgang Bicker,<sup>||,⊥</sup> Bernd R. Binder,<sup>†</sup> and Valery Bochkov<sup>†</sup>

Institute of Vascular Biology and Thrombosis Research, Medical University of Vienna, Schwarzspanierstrasse 17, A-1090 Vienna, Austria, Shimadzu Biotech, Wharfside, Trafford Wharf Road, Manchester M17 1GP, England, Institute of Molecular Pathology, Faculty of Military Health Sciences, University of Defence, Trebesska 1575, CZ-50001 Hradec Kralove, Czech Republic, and Department of Analytical Chemistry, University of Vienna, Währinger Strasse 38, A-1090 Vienna, Austria

6-Aza-2-thiothymine (ATT) is introduced as novel matrix system for the analysis of oxidized phospholipids (OxPLs) by matrix-assisted laser desorption/ionization mass spectrometry (MALDI-MS). A systematic evaluation comparing different established and novel matrix substances, especially 2,4,6-THAP matrix (Stübiger, G.; Belgacem O. *Anal. Chem.* 2007, 79, 3206–3213) as reference compound for phospholipid analysis, and specific matrix additives was performed. Thereby, ATT turned out to be the reagent of choice for MALDI analysis of major biologically relevant OxPL classes (e.g., OxPC, OxPE, and OxPS) in positive and negative ionization mode. ATT used together with specific chaotropic reagents at low concentration (0.5–2 mM) acting as OxPL ionization enhancers revealed an excellent comatrix system for application with MALDI instrument types employing UV- and Nd:YAG laser systems (337 and 355 nm). Moreover, disposable MALDI targets surfaces with specific physicochemical properties (e.g., metallized glass or polymeric substrates) were revealed as superior over stainless steel in terms of reduced chemical background noise (~10-fold better S/N ratios), increased mass spectral reproducibility, and enhanced sensitivity (LOD ~ 250–500 fg on target). The combination of these parameters offers a significant advantage for highly sensitive OxPL profiling by MALDI-MS of biological samples (e.g., human plasma) at trace levels.

Accumulating evidence suggests that oxidized phospholipids (OxPLs) generated by oxidative stress *in vivo* play an important role as lipid mediators in a multitude of biological actions (e.g., cell signaling in regard to gene expression, apoptosis, and

receptor-mediated events) as well as inducers of pathophysiological processes (e.g., inflammation and atherosclerosis).<sup>1–4</sup> On the other hand, OxPLs have been shown to exert also protective activities including upregulation of antioxidative enzymes and inhibition of inflammation,<sup>5</sup> which makes them possible candidates for the development of future anti-inflammatory therapeutics. The most prominent and best characterized OxPLs are those containing *sn*-1 saturated fatty acids (SAFAs) like palmitic (16:0) or stearic (18:0) acid together with oxidatively modified polyunsaturated fatty acids (PUFAs) located at the *sn*-2 position of the glycerol backbone.<sup>6–8</sup> An interesting finding from the biological point of view was that binding of monocytes to endothelial cells and other actions seems to be affected by the oxidized PUFAs in the *sn*-2 position of the molecules rather than by the structure of the polar headgroup.<sup>9</sup> Therefore, methods allowing reliable detection and quantification of individual OxPL species present in biological samples (e.g., human plasma and tissues) are demanded.

Until now protocols for the analysis of OxPLs are almost exclusively based on liquid chromatography coupled with electrospray ionization (ESI-) mass spectrometry (MS).<sup>10,11</sup> However, despite the more frequent use of this approach, matrix-assisted

- (1) Gargalovic, P. S.; Gharavi, N. M.; Clark, M. J.; Pagnon, J.; Yang, W. P.; He, A.; Truong, A.; Baruch-Oren, T.; Berliner, J. A.; Kirchgessner, T. G.; Lusis, A. J. *Arterioscler. Thromb., Vasc. Biol.* 2006, 26, 2490–2496.
- (2) Berliner, J. A.; Leitinger, N.; Tsimikas, S. J. *Lipid Res.* 2009, 50 (Suppl.), S207–S212.
- (3) Furnkranz, A.; Leitinger, N. *Curr. Pharm. Des.* 2004, 10, 915–921.
- (4) Deigner, H. P.; Hermetter, A. *Curr. Opin. Lipidol.* 2008, 19, 289–294.
- (5) Bochkov, V. N.; Kadl, A.; Huber, J.; Gruber, F.; Binder, B. R.; Leitinger, N. *Nature* 2002, 419, 77–81.
- (6) Watson, A. D.; Leitinger, N.; Navab, M.; Faull, K. F.; Horkko, S.; Witztum, J. L.; Palinski, W.; Schwenke, D.; Salomon, R. G.; Sha, W.; Subbanagounder, G.; Fogelman, A. M.; Berliner, J. A. *J. Biol. Chem.* 1997, 272, 13597–13607.
- (7) Podrez, E. A.; Poliakov, E.; Shen, Z.; Zhang, R.; Deng, Y.; Sun, M.; Finton, P. J.; Shan, L.; Febbraio, M.; Hajjar, D. P.; Silverstein, R. L.; Hoff, H. F.; Salomon, R. G.; Hazen, S. L. *J. Biol. Chem.* 2002, 277, 38517–38523.
- (8) Subbanagounder, G.; Wong, J. W.; Lee, H.; Faull, K. F.; Miller, E.; Witztum, J. L.; Berliner, J. A. *J. Biol. Chem.* 2002, 277, 7271–7281.
- (9) Greenberg, M. E.; Li, X. M.; Gugiu, B. G.; Gu, X.; Qin, J.; Salomon, R. G.; Hazen, S. L. *J. Biol. Chem.* 2008, 283, 2385–2396.
- (10) Watson, A. D. *J. Lipid Res.* 2006, 47, 2101–2111.
- (11) Domingues, M. R.; Reis, A.; Domingues, P. *Chem. Phys. Lipids* 2008, 156, 1–12.

\* Corresponding author. E-mail: gerald.stuebiger@meduniwien.ac.at.

† Medical University of Vienna.

‡ Shimadzu Biotech.

§ University of Defence.

|| University of Vienna.

⊥ Present address: FTC-Forensic-Toxicological Laboratory Ltd., Simmeringer Hauptstrasse 24, A-1110 Vienna, Austria.

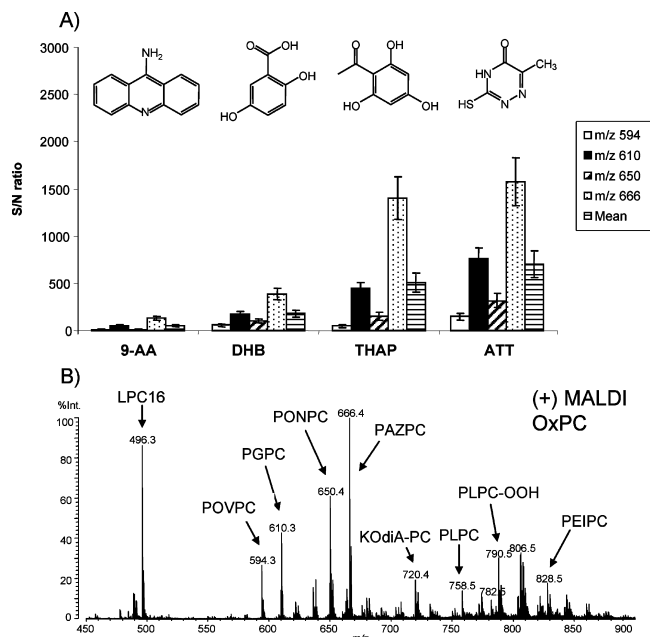


**Figure 1.** Performance of (A) different MALDI matrixes for OxPC detection and (B) detection of individual short- and long-chain OxPC species between  $m/z$  450 and 900 in the positive ionization. A mixture of 125 ng of equivalent amounts of OxPAPC and OxPLPC was recorded. Values are mean  $\pm$  SD of different sample analyses ( $n = 3-4$ ).

laser desorption/ionization mass spectrometry (MALDI-MS) demonstrates several advantages over ESI-MS making it a promising alternative for high-throughput lipid analysis in complex biological samples.<sup>12</sup> In addition to speed of analysis and excellent sensitivity, MALDI-MS is characterized by high tolerance against salts and sample impurities (e.g., anticoagulants, stabilizers, or detergents) and instrumental robustness (e.g., lower susceptibility to instrument contamination and memory effects).<sup>12,13</sup> In spite of these advantages, there are currently no established protocols for the analysis of OxPLs using MALDI-MS available. Thus, methods published for other groups of lipids require critical re-evaluation and significant improvements in order to meet the requirements for detection of the low levels of OxPLs usually present in biological samples. In particular, such methods have to be tolerant to interfering chemical background noise, which is a typical obstacle for sensitive MALDI-MS detection of compounds in the low  $m/z$  range.<sup>14</sup>

The efficiency of ionization in the MALDI process crucially depends on the type of matrix. Therefore, selection of suitable matrixes is a prerequisite for the development of MALDI-MS based analysis methods. Currently, increasing efforts have been made to identify new matrixes and solvent systems for lipid analysis but to date only few matrix substances, e.g., 2,5-dihydroxybenzoic acid (DHB), 4-nitroaniline (PNA), 2,4,6-trihydroxyacetophenone (THAP), and 9-aminoacridine (9-AA) were found to work well for the analysis of diverse lipid classes by

MALDI-MS.<sup>15-18</sup> Nevertheless, the performance of these matrixes for the detection and possible quantitative evaluation of OxPLs at low levels by MALDI-MS has never been tested. 6-Aza-2-thiothymine (ATT) has been reported as a nearly pH-neutral matrix substance allowing the detection of labile molecules, like oligonucleotides,<sup>19</sup> complex N-glycans and glycopeptides,<sup>20</sup> as well as noncovalent protein complexes.<sup>21</sup> Moreover, ATT has more recently been studied for its role as matrix in secondary ionization processes of derivatized peptides analyzed by MALDI.<sup>22,23</sup> These facts attracted our attention to use ATT as a possible matrix substance for the analysis of OxPLs as important group of chemically fragile lipid molecules during our current investigation.

In the present study, we describe an optimized method by introducing ATT as a matrix substance for the highly sensitive detection of OxPLs by MALDI-MS in positive and negative ionization mode. The supplementation of ATT with specific matrix additives (e.g., citrate and chaotropic reagents) led to significantly improved ionization of labile OxPL species (e.g., aldehydic OxPCs) and tolerance to alkali ions usually present in biological samples. The use of disposable MALDI target surfaces (e.g., polymeric metal-coated materials) significantly improved the sensitivity of detection compared to standard stainless steel targets and prevented possible sample cross-contaminations. The excellent sensitivity of the MALDI method in the subpicogram (nanomolar) range allowed the detection of OxPLs at trace levels observed *in vivo*.

## EXPERIMENTAL SECTION

**Lipid Standards and Reagents.** The phospholipid standards used during this study were purchased from Avanti Polar Lipids (Alabaster, AL) and Cayman Chemicals (Ann Arbor, MI), respectively (Table 1). 4-Nitroaniline (PNA), 2,5-dihydroxybenzoic acid (DHB), 2,4,6-trihydroxyacetophenone (THAP), dibasic ammonium citrate (diammonium hydrogen citrate, DAHC), ammonium acetate, as well as Pefablock SC were purchased from Fluka (Buchs, Switzerland). 6-Aza-2-thiothymine (ATT), urea, guanidinium chloride (GUA), and chloroform were purchased from Sigma-Aldrich (Milwaukee, WI). 9-Aminoacridine (9-AA) was obtained from Acros Organics (Morris Plains, NJ). Formic acid (FA), methanol (MeOH), ethanol (EtOH), 2-propanol, and ultrapure water were obtained from Merck (Darmstadt, Germany). All chemicals were obtained in the highest purity grade available. For drying of the MALDI target slides between washing steps exclusively, Pehazell adsorbent cellulose wadding (Paul Hartmann AG, Heldenheim, Germany) was used because of the absence of contamination.

**Oxidation of Native Phospholipids.** Oxidation of native PL standards (e.g., PAPC, PLPC, PAPE, or PAPS) was performed

(12) Schiller, J.; Suss, R.; Arnhold, J.; Fuchs, B.; Lessig, J.; Muller, M.; Petkovic, M.; Spalteholz, H.; Zschornig, O.; Arnold, K. *Prog. Lipid Res.* **2004**, *43*, 449-488.

(13) Zehethofer, N.; Pinto, D. M. *Anal. Chim. Acta* **2008**, *627*, 62-70.

(14) Cohen, L. H.; Gusev, A. I. *Anal. Bioanal. Chem.* **2002**, *373*, 571-586.

(15) Schiller, J.; Arnhold, J.; Benard, S.; Muller, M.; Reichl, S.; Arnold, K. *Anal. Biochem.* **1999**, *267*, 46-56.

(16) Estrada, R.; Yappert, M. C. *J. Mass Spectrom.* **2004**, *39*, 412-422.

(17) Stubiger, G.; Belgacem, O. *Anal. Chem.* **2007**, *79*, 3206-3213.

(18) Sun, G.; Yang, K.; Zhao, Z.; Guan, S.; Han, X.; Gross, R. W. *Anal. Chem.* **2008**, *80*, 7576-7585.

(19) Lecchi, P.; Le, H. M.; Pannell, L. K. *Nucleic Acids Res.* **1995**, *23*, 1276-1277.

(20) Papac, D. I.; Wong, A.; Jones, A. J. *Anal. Chem.* **1996**, *68*, 3215-3223.

(21) Horneffer, V.; Strupat, K.; Hillenkamp, F. *J. Am. Soc. Mass Spectrom.* **2006**, *17*, 1599-1604.

(22) Lecchi, P.; Olson, M.; Brancia, F. L. *J. Am. Soc. Mass Spectrom.* **2005**, *16*, 1269-1274.

(23) Brancia, F. L.; Stener, M.; Magistrato, A. *J. Am. Soc. Mass Spectrom.* **2009**, *20*, 1327-1333.

**Table 1. Nomenclature of the OxPL Standards Used in This Study<sup>a</sup>**

chemical name (abbreviation)	exact mass	R <sub>1</sub>	R <sub>2</sub>	R <sub>3</sub> (headgroup)	supplier
1-palmitoyl-2-hydroxy- <i>sn</i> -glycero-3-phosphocholine (LPC16)	495.33	16:0	OH	choline (PC)	Avanti
1-stearoyl-2-hydroxy- <i>sn</i> -glycero-3-phosphocholine (LPC18)	523.36	18:0	OH	choline (PC)	Avanti
1-palmitoyl-2-(5-oxo-valeroyl)- <i>sn</i> -glycero-3-phosphocholine (POVPC)	593.37	16:0	5:0 (ALDO)	choline (PC)	Avanti
1-palmitoyl-2-glutaroyl- <i>sn</i> -glycero-3-phosphocholine (PGPC)	609.36	16:0	5:0 (COOH)	choline (PC)	Avanti
1-palmitoyl-2-(9-oxo-nonanoyl)- <i>sn</i> -glycero-3-phosphocholine (PONPC)	649.43	16:0	9:0 (ALDO)	choline (PC)	Avanti
1-palmitoyl-2-(5-keto-6-octen-diyl)- <i>sn</i> -glycero-3-phosphocholine (KODiA-PC)	663.37	16:0	8:1 (COOH)	choline (PC)	Cayman
1-palmitoyl-2-azelaoyl- <i>sn</i> -glycero-3-phosphocholine (PAZPC)	665.43	16:0	9:0 (COOH)	choline (PC)	Avanti
1,2-dimyrystoyl- <i>sn</i> -glycero-3-phosphocholine (DMPC)	677.50	14:0	14:0	choline (PC)	Avanti
1-palmitoyl-2-arachidonoyl- <i>sn</i> -glycero-3-phosphoethanolamine (PAPE)	739.52	16:0	20:4	ethanolamine (PE)	Avanti
1-palmitoyl-2-linoleoyl- <i>sn</i> -glycero-3-phosphocholine (PLPC)	757.56	16:0	18:2	choline (PC)	Avanti
1-palmitoyl-2-arachidonoyl- <i>sn</i> -glycero-3-phosphocholine (PAPC)	781.56	16:0	20:4	choline (PC)	Avanti
1-palmitoyl-2-arachidonoyl- <i>sn</i> -glycero-3-phosphoserine (PAPS)	783.51	16:0	20:4	serine (PS)	Avanti

<sup>a</sup> R<sub>1</sub> and R<sub>2</sub> represent the fatty acid residues esterified to the *sn*-1 and *sn*-2 position of the phospholipids backbone. The *sn*-1 acyl groups of OxPLs from biological samples (e.g. human plasma) typically contain saturated fatty acids (SAFAs) between 16 and 18 carbon atoms, e.g., palmitic (16:0) or stearic (18:0) acid. The *sn*-2 acyl groups of short-chain OxPLs contain oxidatively fragmented PUFA residues (e.g., 18:2 or 20:4) typically containing 5–9 carbon atoms with terminal aldehydic (ALDO) or carboxylic (COOH) groups. R<sub>3</sub> corresponds to the headgroups esterified to the *sn*-3 phosphate specifying the corresponding class of molecules. Nomenclature according to the LIPID MAPS classification standard is used ([www.lipidmaps.org](http://www.lipidmaps.org)).

and monitored by mass spectrometry according to the literature.<sup>6</sup> Thereby, mixtures containing the diverse short- and long-chain OxPLs derived from oxidation of the *sn*-2 PUFAs (e.g., OxPAPC, OxPLPC, OxPAPE, and OxPAPS) are obtained.<sup>24</sup> The samples were resuspended in chloroform and stored under argon at –70 °C until ESI- and MALDI-MS analysis.

**Human Plasma Samples.** Human plasma from patients with familial hypercholesterolemia, which are characterized by specific mutations of the LDL receptor (LDL-R) gene and markedly elevated plasma concentrations of low density lipoprotein (LDL) and total cholesterol ranging from 190 to >400 mg/dL were provided by the General Hospital of Vienna (Dept. of Pediatrics and Adolescent Medicine, Vienna, Austria). The participation of the study subjects was approved by the ethics committee of the Medical University of Vienna upon written informed consent.

**Lipid Extraction of Human Plasma.** Lipid extraction was performed according to a modified Folch procedure adjusted to small human plasma samples (<100 μL) using a refrigerated benchtop centrifuge (Eppendorf, Germany) operated at +4 °C. Briefly, 50 μL of fresh plasma samples containing 0.01% BHT and 0.5 mM EDTA as antioxidants and 3 mM Pefablock in order to minimize phospholipase activity<sup>25</sup> were used for extraction using 2 mL Safelock tubes (Eppendorf, Germany). A volume of 1.6 mL of CHCl<sub>3</sub>/MeOH = 2:1 was immediately added and mixed vigorously for 1 min. Afterward 1/4 of the organic phase volume (~0.4 mL) of 0.7 M aqueous formic acid was added and mixed vigorously again. The tubes were centrifuged for 5 min at 6000 rpm (+4 °C) in order to separate the solution in two phases, whereby the lower organic phase containing the lipids was carefully recovered, transferred to a new 2 mL tube, and vacuum-dried (SpeedVac, Thermo Fisher Scientific, Waltham, MA). The lipid residue was redissolved in 100 μL of CHCl<sub>3</sub> and transferred to glass vials for storage at –70 °C.

**Isolation of OxPLs Using Microscale Solid-Phase Extraction (μSPE).** μSPE spin-columns containing C18-modified silica (PepClean, Pierce) were used and operated at approximately 1500

rpm (~200g) using a conventional benchtop centrifuge (Eppendorf, Germany). The lipid extract dissolved in CHCl<sub>3</sub> was dried by argon and then redissolved in 500 μL of MeOH/0.2% FA = 70:30 (v/v) (loading buffer). First the columns are activated and equilibrated by 500 μL of pure MeOH followed by an equal volume of the loading buffer, respectively. Afterward the SPE columns are loaded by the lipid extract (500 μL) followed by a 500 μL washing step (W) using the loading buffer in order to remove salts and the majority of hydrophilic LPCs. The next step consists of a single elution by 700 μL of MeOH/0.2% FA = 82:18 (F1) containing the majority of OxPCs, following two consecutive steps using 500 μL of MeOH/0.2% FA = 85:15 (F2) and 500 μL of MeOH/0.2% FA = 98:2 (F3) containing the unoxidized PCs (see Figure 5A). Finally, the columns are reconstituted by 500 μL of 2-propanol and 500 μL of MeOH in order to remove all residual lipids from the columns, which are then ready again for further use. The SPE fractions were vacuum-dried (SpeedVac, Thermo Fisher Scientific, Waltham, MA) and flushed by argon for storage at –70 °C.

**LC–ESI Mass Spectrometry.** ESI mass spectra were acquired on a PE Sciex API 365 triple quadrupole mass spectrometer (PE Sciex Instruments, Thornhill, Canada) equipped with a pneumatically assisted electrospray ion source and using Analyst 1.4.2 for instrument control. LC–MS analysis was carried out by an 1100 series HPLC system (Agilent Technologies, Waldbronn, Germany) using 10 mM ammonium acetate (= eluent A) and MeOH containing 10 mM ammonium acetate (= eluent B) as solvents. A binary gradient from 80% up to 100% eluent B over 30 min and then back to 80% eluent B within the following 15 min using a Phenomenex Luna C8(2), 3 μm, 100 Å, 150 mm × 2.0 mm i.d. column was used for OxPL separation. MS experiments were performed in positive ionization mode using OxPAPC and OxPAPE as well as in negative ionization mode using OxPAPS as standards, respectively. Full scan analysis (*m/z* range 400–900, flow rate 700 μL/min using an approximately 1:50 flow splitter) and multiple reaction monitoring (MRM) (flow rate 200 μL/min using an approximately 1:20 flow splitter) were employed. MRM was performed for structural confirmation by recording specific transitions of selected OxPL precursor ions. The following transitions were monitored: OxPCs ([M + H]<sup>+</sup> → *m/z* 184, phosphocholine group), OxPEs (fragment ions formed by loss

(24) von, S. E.; Oskolkova, O. V.; Schabbauer, G.; Gruber, F.; Bluml, S.; Genest, M.; Kadl, A.; Marsik, C.; Knapp, S.; Chow, J.; Leitinger, N.; Binder, B. R.; Bochkov, V. N. *Arterioscler. Thromb., Vasc. Biol.* **2009**, *29*, 356–362.

(25) Davis, B.; Koster, G.; Douet, L. J.; Scigelova, M.; Woffendin, G.; Ward, J. M.; Smith, A.; Humphries, J.; Burnand, K. G.; Macphee, C. H.; Postle, A. D. *J. Biol. Chem.* **2008**, *283*, 6428–6437.

of 141 Da, i.e., loss of phosphoethanolamine), and OxPSs (fragment ions formed by loss of 87 Da, i.e., loss of phosphoserine). Lipid samples were dissolved in MeOH/10 mM ammonium acetate = 80:20 (v/v), and approximately 30–50  $\mu$ L were injected for full scan and MRM analysis, respectively.

**MALDI Sample Preparation.** PNA was dissolved in MeOH at a concentration of 10 mg/mL.<sup>16</sup> The matrixes DHB and ATT (each 10 mg/mL) were dissolved in EtOH/water (90:10, v/v) adopted from the literature.<sup>26,27</sup> THAP (10 mg/mL) was dissolved in MeOH/water (70:30, v/v). 9-AA matrix (10 mg/mL) was dissolved in isopropanol/acetonitrile (60:40, v/v) according to the literature.<sup>18</sup> The matrix additives were prepared as 1 M aqueous stock solutions and were added in the range of 0.5–100 mM to the matrix solutions. In general, 0.5  $\mu$ L of the matrixes immediately followed by the same volume of lipid samples (dissolved in pure MeOH or MeOH/water 80:20, v/v) were deposited on the MALDI sample targets without any premixing (dried-droplet technique).<sup>28</sup>

**MALDI Target Surfaces.** For the MALDI sample preparation using the AXIMA-CFRplus platform the following target surfaces were used: (a) FlexiMass (FLEX) stainless steel slides and (b) FlexiMass-DS (FLDS) conductive polymeric metal-coated slides (Shimadzu Biotech, Manchester, U.K.), (c) QuickMass (NANO) nonporous germanium coated glass slides (NanoHorizons, Bellefonte, PA), (d) conductive indium–tin-oxide (ITO) coated glass slides (Prazisions Glas & Optik GmbH, Iserlohn, Germany), and (e) DropStop (DRSP) polymeric aluminized multilayer surface (Schur Inventure, Vejle, DK). All slides were inserted into the MALDI mass spectrometer via specific target adaptors (Adapt/ion and AXIMA-Precision, Shimadzu Biotech) suitable for carrying up to four sample plates in microscopic slide format, simultaneously. The slides could be directly analyzed without modifications, except for the DropStop surface, which was mounted onto FlexiMass slides using double-sided adhesive Scotch tapes (3M, St. Paul MN). The integrity of the field in the extraction region was maintained by ensuring contact of the (conductive) DRSP film on the bulk material of the metal sample holder. In order to verify contact, we measured the continuity between the film and the sample plate using a multimeter. Furthermore, we observed no deteriorating effects especially when considering that DRSP used this way provided by far the best results for OxPL detection in terms of peak resolution and obtained S/N ratios. For the 4800 Proteomics Analyzer MALDI-time-of-flight (TOF)/TOF instrument, standard stainless steel targets containing 16  $\times$  24 sample spots were used.

**MALDI Mass Spectrometry.** All mass spectra shown were obtained using an AXIMA-CFRplus (Shimadzu Biotech, Manchester, U.K.) curved-field reflectron time-of-flight (RTOF) mass spectrometer equipped with a 337 nm pulsed nitrogen laser (3-ns pulse width). The 4800 Proteomics Analyzer MALDI-TOF/TOF instrument (Applied Biosystems, Framingham, USA) equipped with a 355 nm pulsed Nd:YAG laser (3–7 ns pulse width) and a dual-stage reflectron analyzer was used to acquire the mass

spectrum displayed in Figure S-1B. Measurements were performed either in positive or negative mode using delayed ion extraction for optimized mass resolution. The delay time was adjusted according to the mass range under observation ( $m/z$  400–900) allowing for baseline isotopic mass resolution. The ion acceleration voltage was set to 20 kV on both instruments. Mass spectra were obtained applying a laser energy adjusted up to 5–10% above threshold irradiation according to the manufacturer's nominal scale. An integrated video imaging system ( $\sim$ 25 $\times$  magnification) allows direct observation of the sample spots under investigation. MALDI mass spectra represent the accumulation of 500 and 1000 single laser shots dependent on using the AXIMA-CFRplus and 4800 Proteomics Analyzer instrument, respectively. Mass spectra were calibrated using mixtures of the phospholipid standard compounds described above.

**MALDI-MS Data Analysis.** Processing of MS data was performed by the manufacturer supplied instrument software versions Launchpad 2.8 (Shimadzu Biotech) and Data Explorer v.4.9 (Applied Biosystems) using the Savitzky–Golay smoothing algorithm. MALDI mass spectra were routinely recalibrated using the exact mass values of the standard compounds indicated above. Data evaluation was made by Microsoft Excel 2003 software package. Values are displayed as mean  $\pm$  standard deviation (SD) of at least triplicate measurements ( $n \geq 3$ ).

## RESULTS AND DISCUSSION

**Matrix Comparison for Detection of Different OxPL Classes by MALDI-MS.** Since efficiency of ionization of individual compounds critically depends on the type of matrix, several commercially available MALDI matrix substances were evaluated for the detection of OxPCs. PNA did not provide any useful mass spectra of OxPCs at all, followed by 9-AA showing only lower quality mass spectra and DHB, which provided considerably better results under our experimental setup. On the basis of signal-to-noise (S/N) ratio measurements, a 5–10-fold increase of mean OxPC signals could be observed by using THAP as the matrix, which serves as our reference substance for PL analysis by MALDI-MS.<sup>17</sup> Compared to these matrixes, ATT produced the best mass spectral quality and S/N ratios of OxPCs during our investigation (Figure 1A). In addition, ATT provided qualitatively similar mass spectra of OxPCs obtained from different MALDI-TOF instruments using laser types emitting at 337 and 355 nm, respectively (Figure S-1 in the Supporting Information). Thereby, MALDI mass spectra recorded in the range between  $m/z$  450 and 900 simultaneously displays the major types of OxPCs present in biological samples: (a) long-chain OxPCs containing oxidized but nonfragmented *sn*-2 PUFA residues in the range  $> m/z$  758–782 (i.e., the PLPC and PAPC precursors), (b) short-chain aldehydic or carboxylic OxPCs (e.g.,  $m/z$  594, 610, 650, 666) containing fragmented oxidized *sn*-2 PUFAs in the range between  $m/z$  550–740, and (c) LPC16 ( $m/z$  496) as the major fragmentation product of OxPCs (Figure 1B). An interesting finding was that by measuring the individual OxPC standards (see Table 1), a clear difference in the contribution of LPC16 ( $m/z$  496) to the mass spectra in the order: 9-AA > DHB > THAP > ATT was observed indicating for different degree of OxPC fragmentation during the ionization process (Figure S-2 in the Supporting Information). Thereby, aldehydic OxPCs (e.g., POVPC) compared to carboxylic OxPCs (PGPC, KOdiA-PC) and unoxidized PCs (e.g., DMPC)

(26) Krause, J.; Stoeckli, M.; Schlunegger, U. P. *Rapid Commun. Mass Spectrom.* **1996**, *10*, 1927–1933.

(27) Dashtiev, M.; Wafler, E.; Rohling, U.; Gorshkov, M.; Hillenkamp, F.; Zenobi, R. *Int. J. Mass Spectrom.* **2007**, *268*, 122–130.

(28) Kussmann, M.; Nordhoff, E.; Rahbek-Nielsen, H.; Haebel, S.; Rossel-Larsen, M.; Gobom, J.; Mirgorodskaya, E.; Kroll-Kristensen, A.; Palm, L.; Roepstorff, P. *J. Mass Spectrom.* **1997**, *32*, 593–601.

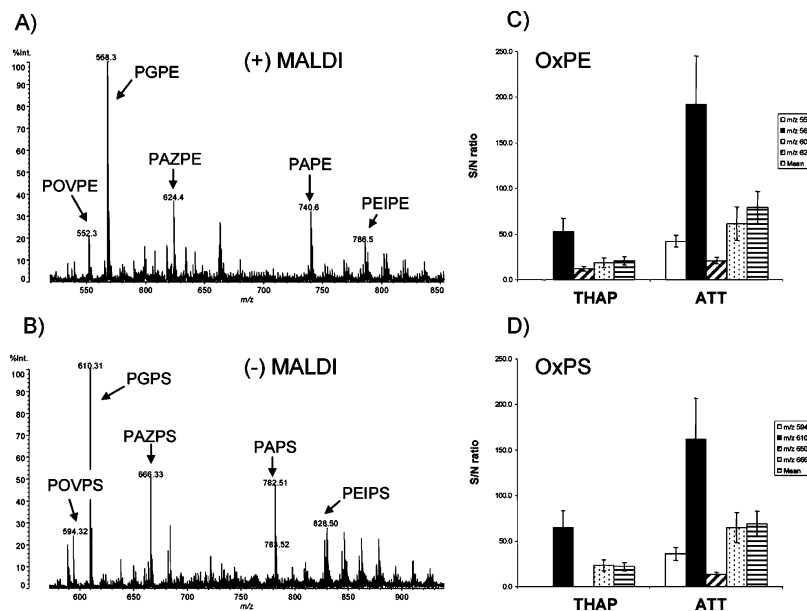


**Figure 2.** MALDI mass spectra of (A) OxPEs recorded in positive and (B) OxPSs detected in negative mode. The ionization efficiency of (C) individual short-chain OxPE and (D) OxPS species detected on standard THAP compared to the novel ATT matrix based on measurement of the S/N ratios in the corresponding ionization modes is shown. A total of 50 ng of equivalent amounts of OxPAPE and OxPAPS were analyzed. Values are mean  $\pm$  SD of different sample analyses ( $n = 3-4$ ).

appeared to be especially prone to LPC formation during ionization using the different matrix substances. In this context, compared to the other evaluated matrixes, ATT was revealed as the “softest” matrix substance for the analysis of OxPLs in terms of producing the lowest amount of LPC during the ionization process.

Beside application to OxPCs, we tested the suitability of ATT also for detection of other biologically abundant OxPL classes, namely, oxidized PE (OxPE) and PS (OxPS). It is known that ionization of PLs mainly depends on the polar headgroups bearing different functional groups. Consequently, because of the fixed positive charge of the choline headgroup, OxPCs are exclusively detectable in positive mode using MALDI-MS, OxPEs can be recorded in both modes, and OxPSs are detected favorably as negative ions because of the negative charge of the serine headgroup. Thereby, the  $m/z$  values of OxPEs have a nominal mass difference of  $-42$  u recorded in the positive mode and OxPSs detected in the negative mode show the same values to OxPCs recorded in the positive mode, respectively. As compared to OxPC, the MALDI mass spectra of OxPE and OxPS display all the essential OxPL species derived from oxidation of PAPE and PAPS, respectively. As can be seen in Figure 2, the application of ATT matrix induced a significant increase of S/N ratios of these individual OxPL species when compared to THAP standard matrix. Comparison of MALDI mass spectra recorded on ATT matrix with those obtained from ESI-MS of the same samples during a recently published study showed a high degree of similarity in terms of the number of individual OxPC species and their relative signal intensity.<sup>24</sup> Thus, all together these results clearly demonstrate that ATT matrix is a versatile and sensitive reagent for the quantitative detection of the different OxPL classes by MALDI-MS.

**Effects of Chaotropic Matrix Additives on Detection of Different OxPL Classes.** Defined matrix additives (i.e., comatrixes) are often used in order to improve the overall MALDI performance, especially for the analysis of chemically labile

analytes (e.g., oligonucleotides and phosphopeptides).<sup>29,30</sup> Therefore, we expanded our matrix evaluation on the use of different ATT comatrixes including certain monosaccharides (e.g., fucose),<sup>29</sup> diammonium hydrogen citrate (DAHC),<sup>17</sup> and chaotropic reagents like urea or guanidinium chloride (GUA), which have been shown to improve the solubility of phospholipids in aqueous solutions.<sup>31</sup>

In general, the formation of multiple alkali adduct ions reduces sensitivity of detection due to signal splitting and is one of the major obstacles for the reliable quantitative evaluation of MALDI mass spectra of lipids derived from biological samples.<sup>32</sup> We observed considerable differences in the degree of alkali adduct formation (mainly  $[M + Na]^+$  ions) between individual OxPCs on the different matrix systems (Figure S-3 in the Supporting Information). Instead, with the use of DAHC as an ATT matrix additive,  $[M + Na]^+$ ,  $[M + K]^+$ , and  $[M + 2Na - H]^+$  ions could be effectively reduced to  $<10\%$  of the total signal intensity of individual OxPC species in favor of predominant  $[M + H]^+$  even in the case of samples containing higher sodium concentrations ( $>10$  mM) (Figure S-4 in the Supporting Information).

In contrast, although effectively preventing alkali adduction, use of DAHC as a comatrix alone could not essentially improve the detection of chemically labile OxPCs (e.g., POVPC, PONPC, PEIPC) (Figure 3). On the other hand, addition of urea or GUA clearly improved the ionization efficiency of OxPLs in a matrix and concentration dependent manner. During our investigation, the optimum concentrations of GUA and urea were found in the range between 0.5 and 2 mM, whereby both worked best when used together with the ATT matrix (Figure S-5 in the Supporting Information). In the case of OxPE and OxPS, the addition of

(29) Distler, A. M.; Allison, J. *Anal. Chem.* **2001**, *73*, 5000–5003.

(30) Kjellstrom, S.; Jensen, O. N. *Anal. Chem.* **2004**, *76*, 5109–5117.

(31) Oku, N.; MacDonald, R. C. *J. Biol. Chem.* **1983**, *258*, 8733–8738.

(32) Zschornig, O.; Richter, V.; Rassoul, F.; Süss, R.; Arnold, K.; Schiller, J. *Anal. Lett.* **2006**, *39*, 1101–1113.

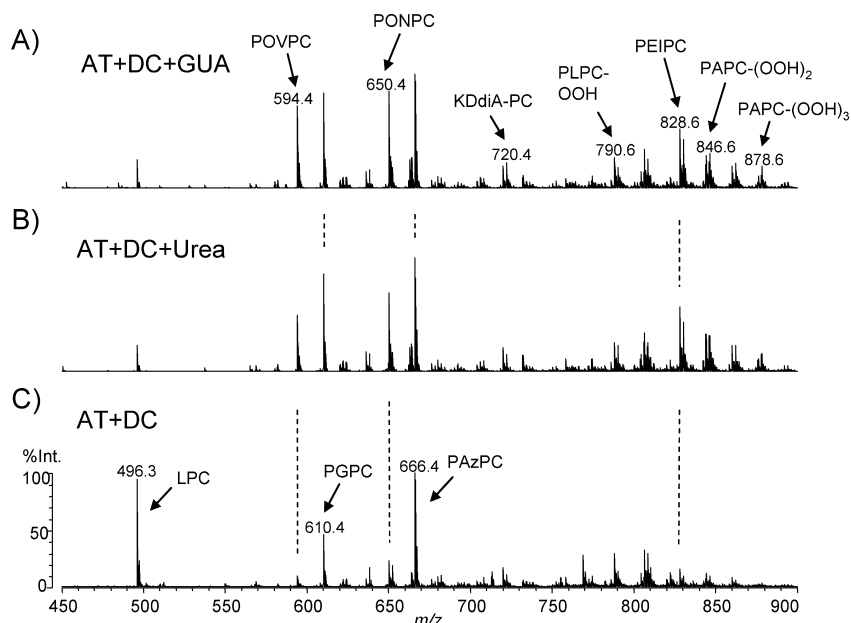


**Figure 3.** MALDI mass spectra of OxPCs recorded on ATT matrix using (A) DAHC + GUA, (B) DAHC + urea, and (C) DAHC alone as matrix additives, respectively. A mixture of 50 ng of equivalent amounts of OxPAPC and OxPLPC was analyzed. As matrix additives, 20 mM DAHC and 1–2 mM of the chaotropic reagents were used for the measurements (for details, see the text).

DAHC provided effective suppression of  $[M + Na]^+$ ,  $[M + 2Na - H]^+$  and  $[M - 2H + Na]^-$  ions, which are normally much more prominent than in mass spectra of PC recorded by MALDI- or ESI-MS<sup>33,34</sup> because of the higher affinity for alkali ions of these lipid classes. In accordance to our observations with OxPC, a clear increase in S/N ratios of individual short-chain OxPE and OxPS could also be observed using the chaotropic reagents as an ATT matrix additive (Figure S-6 in the Supporting Information). In general, taking together the results of our evaluation, GUA appeared to be the most effective and universal comatrix reagent in order to enhance the stability and improve the detection of OxPLs by MALDI-MS.

**Influence of Disposable MALDI Target Surfaces on OxPL Detection.** Because MALDI is a surface-based technique, one of the major factors contributing to mass spectral quality and sensitivity of detection is the contribution of chemical background noise originating from the target surface.<sup>35</sup> It has recently been shown that alternative MALDI substrates (e.g., nonporous silicone, graphite, or Teflon surfaces) can considerably increase sensitivity via several mechanisms comprising reduced background noise, sample spot concentration, and enhanced ionization efficiency.<sup>36</sup> Hence, we assume that the chemical background noise can be attributed to (a) alkali ions present in the surface, (b) laser-desorption/ionization (LDI) background signals from the surface material, and (c) signals produced by the MALDI matrix itself (i.e., matrix background). Moreover, among the physicochemical differences, the roughness of the material seems to play a crucial role<sup>37</sup> for the retention of low-mass contaminants, especially after repeated usage of the same surface, thus further contributing to the chemical noise.

In the present work, we compared stainless steel with several disposable alternative MALDI targets surfaces in terms of their contribution to chemical background noise and ionization efficiency of OxPLs under application of the novel ATT comatrix system. In general, the chemical noise detected on these surfaces was only 2–20% of that observed using stainless steel targets. Major differences in the contribution of alkali ( $Na^+$ ,  $K^+$ ) and of matrix cluster ions were observed on the different surfaces, whereby stainless steel produced the most intense background noise in the MALDI mass spectra (Figure S-7 in the Supporting Information). Applied to the analysis of selected short-chain OxPCs, 5–7 times better mean S/N ratios were obtained compared to the stainless steel target (Figure 4A). During our evaluation the hydrophobic DRSP surface<sup>38,39</sup> provided the overall best performance in terms of very low chemical background noise, spot-to-spot reproducibility, and S/N ratio of OxPCs (Table 2). This surface provided 40–60% more concentrated sample spots after solvent evaporation compared to all the other ones. The limit of detection (LOD) of individual short-chain OxPCs standards measured on DRSP was found below 250–500 fg on target, which was >5 times lower as compared to stainless steel targets where the LOD was found in the range of >1 pg/ $\mu$ L (Figure 4B). These effects can be explained by the concentration of sample spots during matrix crystallization and the improved ionization efficiency of OxPCs on the DRSP surface. A summary of the performance characteristics of the different MALDI target surfaces is provided in Table 2.

**Application of the Novel MALDI Approach on OxPL Detection *in Vivo*.** The trace levels of individual OxPLs ( $\sim$ 0–2  $\mu$ M) expected to be present *in vivo* (e.g., human plasma)<sup>40</sup> demands highly sensitive detection especially because MALDI-

(33) Stubiger, G.; Pittenauer, E.; Allmaier, G. *Anal. Chem.* **2008**, *80*, 1664–1678.

(34) Hsu, F. F.; Turk, J. J. *Am. Soc. Mass Spectrom.* **2005**, *16*, 1510–1522.

(35) Krutchinsky, A. N.; Chait, B. T. *J. Am. Soc. Mass Spectrom.* **2002**, *13*, 129–134.

(36) Kim, J. K.; Murray, K. K. *Rapid Commun. Mass Spectrom.* **2009**, *23*, 203–205.

(37) Okuno, S.; Arakawa, R.; Okamoto, K.; Matsui, Y.; Seki, S.; Kozawa, T.; Tagawa, S.; Wada, Y. *Anal. Chem.* **2005**, *77*, 5364–5369.

(38) Rechthaler, J.; Allmaier, G. *Rapid Commun. Mass Spectrom.* **2002**, *16*, 899–902.

(39) Stubiger, G.; Marchetti, M.; Nagano, M.; Reichel, C.; Gmeiner, G.; Allmaier, G. *Rapid Commun. Mass Spectrom.* **2005**, *19*, 728–742.

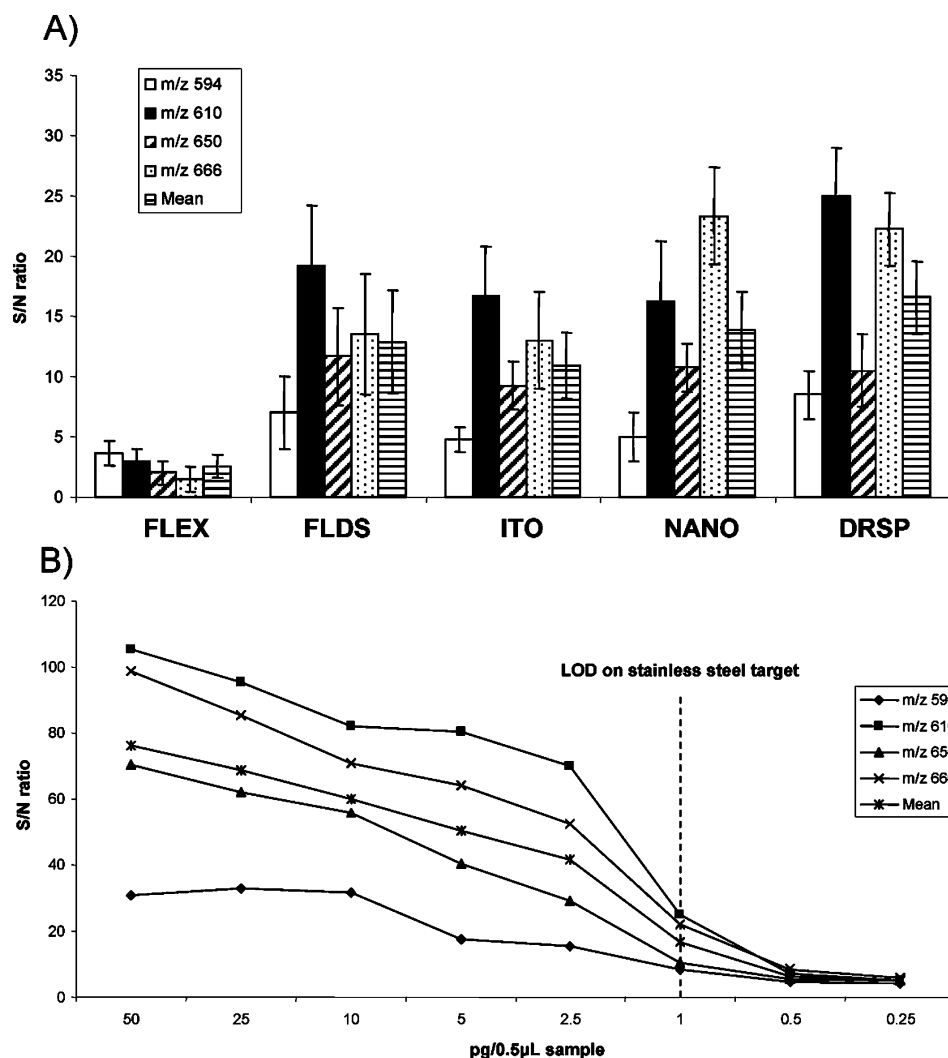


**Figure 4.** Comparison of (A) the ionization efficiency of different MALDI target surfaces and (B) the concentration dependence of short-chain OxPC signal intensity on DRSP surface based on S/N ratio measurements. Equivalent mixtures of the individual OxPC standards described in Table 1 were analyzed. Values are mean  $\pm$  SD of four different sample analyses ( $n = 4$ ). FLEX, stainless steel slides; FLDS, polymeric slides; NANO, nonporous germanium coated glass slides; ITO, conductive indium–tin-oxide coated glass slides; DRSP, polymeric aluminized multilayer surface.

**Table 2. Performance of the Different MALDI Target Surfaces for OxPC Detection<sup>a</sup>**

	FLEX	FLDS	ITO	NANO	DRSP
spot diameter <sup>b</sup>	1658 $\pm$ 53	1663 $\pm$ 78	1967 $\pm$ 119	1988 $\pm$ 279	1260 $\pm$ 70
alkali ions <sup>c</sup>	900 $\pm$ 225	20 $\pm$ 6	20 $\pm$ 3	140 $\pm$ 32	8 $\pm$ 2
LDI background <sup>d</sup>	7 $\pm$ 1.8	3 $\pm$ 0.8	1 $\pm$ 0.23	20 $\pm$ 6	0.1 $\pm$ 0.02
matrix background <sup>e</sup>	180 $\pm$ 54	20 $\pm$ 7	70 $\pm$ 27	60 $\pm$ 18	10 $\pm$ 3
total chemical noise <sup>f</sup>	1087 $\pm$ 281	43 $\pm$ 18	91 $\pm$ 30	220 $\pm$ 56	18 $\pm$ 5
LOD (S/N $\geq$ 3)	1 pg	500 fg	250–500 fg	500 fg	250 fg
LOQ (S/N $\geq$ 10)	>5 pg	1–2 pg	<1 pg	>1 pg	>500 fg
LPC/OxPC ratio <sup>g</sup>	2.5	2.6	1.6	1.8	1.6
overall surface performance	+	++	++ <sup>h</sup>	++ <sup>i</sup>	+++

<sup>a</sup> The limit of detection (LOD) and limit of quantification (LOQ) based on S/N definition is indicated. Values are mean  $\pm$  SD ( $n = 3–6$ ). FLEX, stainless steel slides; FLDS, polymeric metal-coated slides; NANO, nonporous germanium coated glass slides; ITO, indium–tin-oxide coated glass slides; DRSP, polymeric aluminized multilayer surface. <sup>b</sup> Dried spot diameter on MALDI target (in micrometers) applying 1  $\mu$ L of sample and ATT matrix on the surface. <sup>c</sup> Peak intensity (millivolts) of sodium ( $m/z$  23) and potassium ( $m/z$  39) ions. <sup>d</sup> LDI signals derived from the plain surfaces. <sup>e</sup> ATT matrix signals in the  $m/z$  range 450–900. <sup>f</sup> Representing the sum of the values from alkali ions, LDI background, to matrix background. <sup>g</sup> Calculated based on the signal-to-noise ratio (S/N) of LPCs and OxPCs recorded on the different surfaces. <sup>h</sup> Intense background peaks visible applying low sample amounts (<1 pg). <sup>i</sup> Reduced sample spot reproducibility due to matrix diffusion effects during crystallization: +, useful; ++, good; +++, excellent.

MS is usually restricted to the application of small sample volumes (0.5–1  $\mu$ L) for analysis. With the comparison of the absolute LODs (~500 pg–1 ng/mL) obtained by the different MALDI sample supports described above with total OxPC levels found in human

plasma (up to ~400 ng/mL),<sup>40</sup> the MALDI technique shows the potential for OxPC detection at trace levels *in vivo*. Nevertheless, because of the high abundance of unoxidized PLs in biological samples, chromatographic separation of OxPLs is usually needed

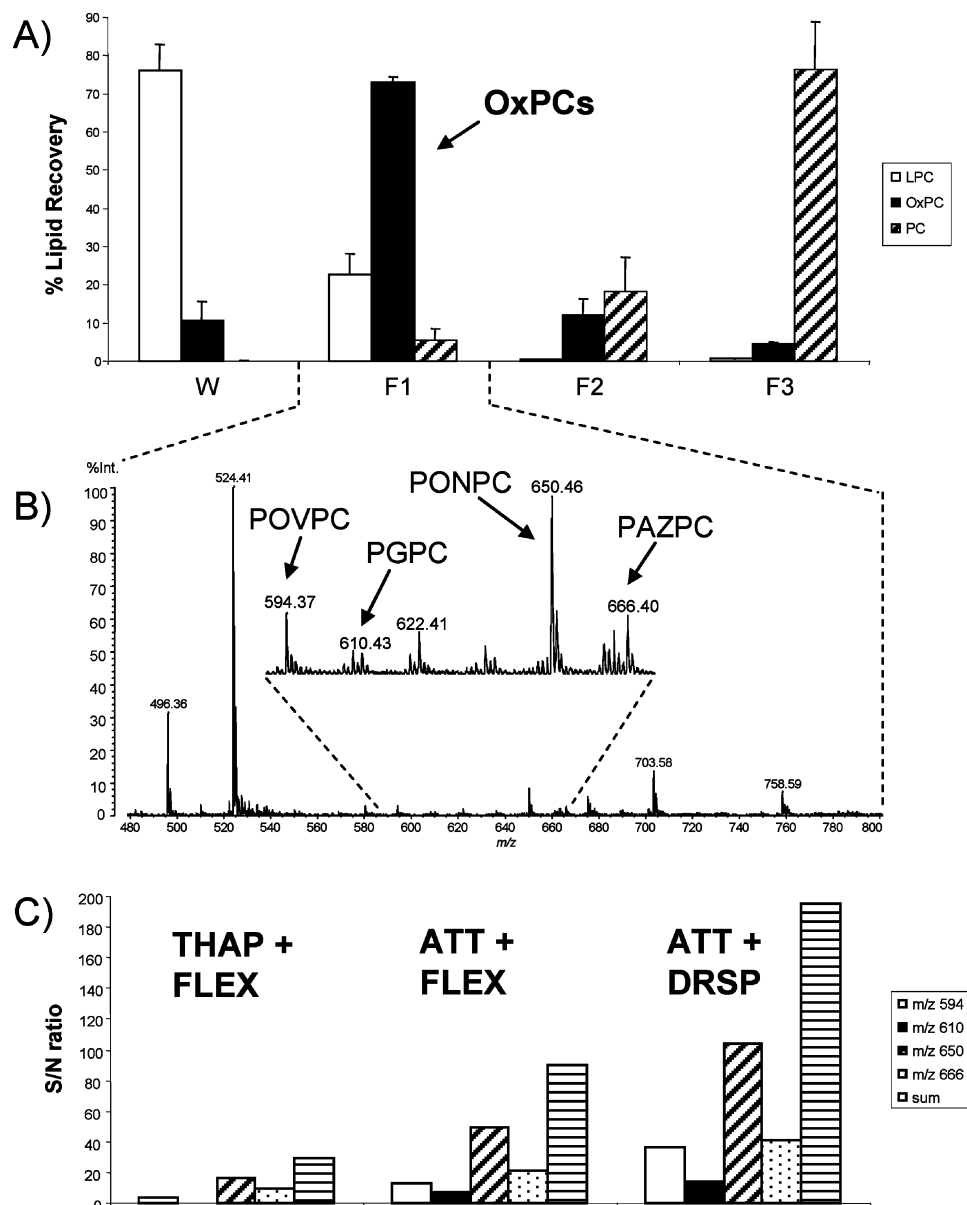


**Figure 5.** Detection of short-chain OxPCs from human plasma sample *in vivo*. In part A, the performance of the  $\mu$ SPE method in terms of the separation efficiency of OxPCs from LPCs and unoxidized PCs based on results of LC-ESI-MRM is shown (for details see the Experimental Section). In part B, the MALDI mass spectrum of the  $\mu$ SPE-fraction containing the majority of OxPCs (F1) is shown, and in part C the increase of the S/N ratios of individual short-chain OxPCs detected *in vivo* using standard matrix (THAP) and stainless steel targets (FLEX), compared to using ATT with FLEX and the DRSP surface, is displayed. The lipid extract of 50  $\mu$ L of plasma from a hypercholesterolemic patient was analyzed. Values are mean  $\pm$  SD of four independent analyses of the same plasma sample ( $n = 4$ ).

to minimize analyte suppression effects and to increase the dynamic range of detection.<sup>6,7</sup> To test the application potential of our novel MALDI approach, we have established a microscale solid-phase extraction ( $\mu$ SPE) protocol for rapid separation and enrichment of OxPLs from small amounts of biological samples. The  $\mu$ SPE separation efficiency for OxPLs was assessed via LC-ESI-MRM (Figure 5A) and the corresponding  $\mu$ SPE-fraction containing the majority of OxPLs (fraction F1) was collected and directly analyzed by MALDI-MS as outlined in the Experimental Section. As can be seen in Figure 5B from an experiment using 50  $\mu$ L of human plasma of a hypercholesterolemic patient, a

number of characteristic short-chain OxPC species could be detected in the F1-fraction from  $\mu$ SPE-separation. Thereby, the sensitivity of detection using our novel ATT comatrix system together with disposable target surfaces (e.g., DRSP) instead of using standard matrix (e.g., THAP) and stainless steel (e.g., FLEX) improved the S/N ratio by a factor of  $\sim 10$  (Figure 5C). On the basis of this approach, the short-chain OxPC profile from the patient's sample was found in the order: PGPC ( $m/z$  610) < POVPC ( $m/z$  594) < PAZPC ( $m/z$  666) < PONPC ( $m/z$  650). This indicates for the prevalence of oxidation products derived from PLPC (i.e.,  $m/z$  650 and 666), which is the most abundant PUFA-containing PC present in human plasma.<sup>41</sup> In an attempt to estimate the corresponding amounts of OxPCs based on measure-

(40) Podrez, E. A.; Byzova, T. V.; Febbraio, M.; Salomon, R. G.; Ma, Y.; Valiyaveetil, M.; Poliakov, E.; Sun, M.; Finton, P. J.; Curtis, B. R.; Chen, J.; Zhang, R.; Silverstein, R. L.; Hazen, S. L. *Nat. Med.* **2007**, *13*, 1086–1095.

(41) Myher, J. J.; Kuksis, A.; Pind, S. *Lipids* **1989**, *24*, 408–418.

ment of S/N ratios using the DRSP surface (see Figures 4B and 5C), the amounts of individual short-chain OxPCs were found between  $\sim 1$  and 125 ng/mL and  $\sim 100$  and 250 ng/mL of total short-chain OxPCs in the human plasma sample, which matches the range of recently published data.<sup>40</sup>

Following a separate *in vitro* time-course experiment of OxPC formation (Figure S-8 in the Supporting Information), a significant signal intensity increase relative to the PUFA-containing precursor species (i.e., PLPC and PAPC) in the order PAZPC ( $m/z$  666) < PONPC ( $m/z$  650) < POVPC ( $m/z$  594) < PGPC ( $m/z$  610) could be observed during lipid auto-oxidation *in vitro*. Interestingly, despite the predominant generation of PGPC *in vitro* the relative abundance of aldehydic OxPCs (e.g., POVPC, PONPC) was found to be higher *in vivo* as might have been expected from the lipid auto-oxidation experiment. In view of these interesting findings, results of a more detailed study including clinical samples will be provided in another publication.

## CONCLUSIONS

Lipid analysis by MALDI-MS still represents an active and dynamic area of research. The discovery of novel matrix substances and constant improvements in sensitivity and reproducibility opens the possibility for the setup of novel lipidomics approaches. During our investigation, the application potential of MALDI-MS was extended toward the analysis of OxPLs as a group of labile lipid metabolites and potential disease markers. The detailed evaluation of critical parameters including different matrix substances, specific additives (e.g., chaotropic reagents), and alternative MALDI sample supports (e.g., hydrophobic polymeric metal-coated surfaces) revealed crucial to obtain sufficiently high sensitivity and versatility for detection of different OxPL classes in positive and negative ionization mode. Especially, the introduction of ATT matrix for this specific application considerably

improved the mass spectral quality in terms of reduced fragmentation and increased sensitivity of detection (picogram to femtogram range). Finally, the combination of these essential factors allowed the detection and quantification of OxPLs from small amounts of biological samples (e.g., human plasma) showing clear differences in the OxPC profile compared to *in vitro* auto-oxidation. Considering the robustness and high-throughput capability of MALDI-MS in general, our novel approach represents a promising platform for clinical screenings of lipid biomarkers in the future.

## ACKNOWLEDGMENT

G.S. and O.B. contributed equally to this work. The authors thank Olga Oskolkova for performing the lipid oxidation experiments and Michael Wuczowski for microscopic evaluation of the MALDI surface preparations. Prof. Wolfgang Lindner is acknowledged for provision of ESI-MS instrument time and Prof. Kurt Widhalm for his continuous support. Further we would thank Kenneth MacAskill for careful reading of the manuscript. We gratefully acknowledge the contribution of Shimadzu Biotech for providing the MALDI instrumentation, without which this work could not have been accomplished. This work was financially supported by FFG Research Grant No. 815445 (to V.B.) and by the Institutional Research Plan No. MO0FVZ0000501 from the Faculty of Military Health Sciences, University of Defence, Czech Republic.

## SUPPORTING INFORMATION AVAILABLE

Additional information as noted in the text. This material is available free of charge via the Internet at <http://pubs.acs.org>.

Received for review February 1, 2010. Accepted May 10, 2010.

AC100280P